ARTICLE

OBC
www.rsc.org/obc

Use of an adjustable soft segment as an effective molecular design for crystal engineering of hydrogen-bonded tape motifs †

Ryoichi Takasawa, Isao Yoshikawa and Koji Araki*
Institute of Industrial Science, University of Tokyo, 4-6-1 Komaba, Meguro-ku, Tokyo 153-8505, Japan

Received 3rd December 2003, Accepted 1st March 2004
First published as an Advance Article on the web 18th March 2004

From all the 11 alkylsilylated guanosine and adenosine derivatives having different numbers and types of nonpolar and flexible alkylsilyl side chains, 13 crystals were obtained from appropriate solvents in spite of their low molecular symmetry, and their crystal structures were studied by X-ray crystallography and thermal analysis. In these crystals, a clear structural hierarchy was observed, and one-dimensional tape motifs were preferentially formed by multiple inter-base hydrogen bonds. The tape motifs were arranged in lamellar-like (**L**), herringbone (**H**) or widened lamella (**WL**) structures in the crystals. However, the alkylsilylated ribose unit adopted a variety of conformations with notable disorders at the alkylsilyl moiety. These results suggested that role of the adjustable and nonpolar alkylsilyl ribose unit was to provide cushioning or a filling effect as a molecular pad, which assisted the crystal packing of the robust tape motifs. The packing mode of the tape motifs could be understood from the size instead of the shape of the adjustable alkylsilyl ribose moiety, offering a novel approach to their crystal engineering.

Introduction

Rational design and syntheses of novel crystalline materials with desirable physical attributes such as electrical, optical, and magnetic properties are the subject of intense studies.[1] To achieve this goal, the design of molecular functionality alone is not adequate, since specific solid-state properties depend on the relative arrangement and orientation of the component molecules. However, the packing arrangements of three-dimensional crystal structures at the molecular level are difficult to predict and control because of the interplay of various thermodynamic and kinetic contributions during the process of nucleation.[2] To this end, one of the most promising approaches is the hierarchical construction of the crystal structure.[3] In this strategy, reliable one- or two-dimensional predefined and self-assembled aggregates in mesoscopic-scale such as tape, ribbon, and sheet motifs are used as building blocks to limit the number of possible molecular arrangements in the three-dimensional crystal structure.[4] Multiple hydrogen bonds are most frequently used as the principal interaction to form the motifs because of their high stability and directionality, and various hydrogen-bonded motifs have been studied.[5] However, multiple hydrogen-bond formation requires a strict spatial arrangement of the component molecules. Since closest packing is required for crystallisation of neutral organic molecules, a small difference in molecular and motif shapes not only alters the mode of the motif packing, but also prevents crystal packing, thus making prediction of the crystal structure from the molecular level a distant goal. To overcome or circumvent this difficulty, various attempts to predict or control the mode of the hydrogen-bonded motif packing in crystals have been actively made. Those include the use of symmetrical molecules or motifs,[6] the introduction of chirality,[7] directional control of interaction,[8] or extensive and large-scale molecular mechanics and dynamics simulation.[9] Here, we will show that use of an adjustable soft segment is an effective approach for this purpose.

Nucleosides are excellent molecules for the construction of supramolecular architectures because of their high inter-base hydrogen-bonding ability and conformational diversity. Multiple hydrogen bonds between base moieties of nucleosides lead to the formation of rigid and stable complementary base pairs,[10] one-dimensional tapes,[11,12] ribbons,[13] two-dimensional sheets,[14] or cyclic tetramers,[15] while ring conformations of the ribofuranose and rotation along the *N*-glycosyl bond offer great conformational diversity.[16] Supramolecular assemblies of alkyl-substituted nucleosides have been actively studied by Gottarelli and his group.[12,13,15b,c] We have also successfully fabricated nucleoside-based gels,[14a] fibers[11] and films[14b] by the introduction of nonpolar and flexible alkylsilyl groups to the ribose or deoxyribose moieties. Some of the crystal structures of the alkylsilylated nucleosides have also been reported.[11,14a,17] In these supramolecular assemblies, the hierarchical structures composed of the hydrogen-bonded tape or sheet motifs were recognised. We extended this hierarchical strategy further to crystal engineering, and studied the packing mode of the hydrogen-bonded tape motifs of alkylsilylated nucleoside derivatives in their crystals. The nonpolar and flexible nature of the alkylsilyl groups and the highly adjustable nature of nucleoside conformation might offer a buffer or a filling effect, and relieve the effect of the small difference of molecular shape onto crystal packing. In this study, we prepared a series of nucleoside derivatives having different numbers and sizes of nonpolar alkylsilyl groups as the adjustable soft segment, crystallised them from appropriate solvents, and studied their structures. Through these studies, we will show that a novel molecular design using the adjustable soft segment as a molecular pad for crystal packing is an effective method for understanding and possibly predicting the packing mode of the robust hydrogen-bonded tape motifs.

Results

Molecular design and crystal formation

One-dimensional tape motifs formed by double inter-base hydrogen bonds are frequently found in the crystals of nucleobase derivatives.[18–21] In the case of guanine and adenine derivatives, the base arrangement within the tape motif is tightly fixed by double inter-base hydrogen bonds (Fig. 1). The inter-base distance (*d*) of the guanine derivatives along the tape

† Electronic supplementary information (ESI) available: figures of tape motifs and table of hydrogen bond distances for alkylsilylated nucleoside crystals. See http://www.rsc.org/suppdata/ob/b3/b315769e/

DOI: 10.1039/b315769e

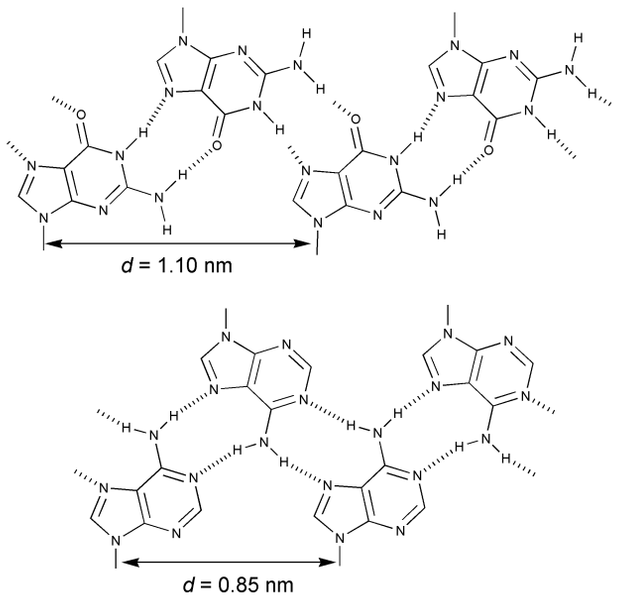

Fig. 1 Hydrogen-bonded tape motifs of guanine and adenine. (Typical inter-base distances (d) of tape motifs in 9-ethylguanine and 9-methyladenine crystal).

direction (typical example: 1.10 nm for 9-ethylguanine[18d]) is slightly longer than that of the adenine derivatives (typical example: 0.85 nm for 9-methyladenine[20o]). To relieve the strict spatial requirement for the packing of the tape motifs at crystallisation, we introduced nonpolar and flexible alkylsilyl groups to the corresponding nucleosides as the adjustable soft segment. Based on this molecular design, we prepared a series of alkylsilylated nucleosides having different sizes of the alkylsilyl moieties. The alkylsilyl groups used in this study were *tert*-butyldiphenylsilyl (TBDPS), triisopropylsilyl (TIPS) and tert-butyldimethylsilyl (TBDMS) groups, and the size is largest for TBDPS and smallest for TBDMS.[22] The compound having TBDPS groups at the 2′ and 3′ positions, 2′,3′-bis-*O*-(tert-butyldiphenylsilyl)guanosine, could not be obtained by selective hydrolysis of 2′,3′,5′-tris-*O*-(tert-butyldiphenylsilyl)guanosine. Thus, eight guanosine derivatives having TBDMS, TIPS or TBDPS and three adenosine derivatives having TBDMS were prepared. Scheme 1 shows the structures and abbreviations of the alkylsilylated nucleosides. The syntheses and crystal structures of some of these compounds have been reported.[11,14a,17] In these compounds, the size of the alkylsilyl moieties and inter-base distance (d) in the tape motif can be tuned by selection of the number and type of the alkylsilyl groups and the type of the nucleobase, respectively. In spite

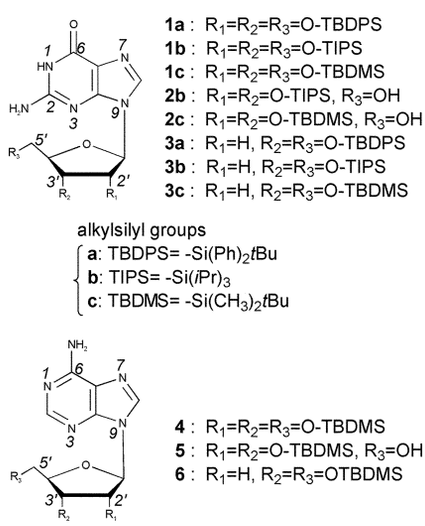

Scheme 1 Alkylsilylated nucleosides.

Table 1 Crystal data and structure refinement for alkylsilylated nucleoside crystals

Crystal data	**1a·MeOH**[a]	**1a·EA**[a]	**1b**	**2b**	**2c·AcOH**[a]	**3c**	**4**	**5**	**6**
Crystallised from	MeOH	Ethyl acetate	EtOH	EtOH	AcOH/EtOH	DMF	EtOH	MeOH	Ethyl acetate/hexane
Molecular formula	C59H71N5 O6Si3	C66H83N5 O9Si3	C37H73N5 O5Si3	C28H53N5 O5Si2	C24H45N5 O7Si2	C22H41N5 O4Si2	C28H55N5 O4Si3	C22H41N5 O4Si2	C22H41N5 O3Si2
Formula weight	1030.48	1174.64	752.27	595.93	571.83	495.78	610.04	495.78	479.78
Crystal system	Monoclinic	Orthorhombic	Monoclinic	Triclinic	Monoclinic	Monoclinic	Monoclinic	Monoclinic	Orthorhombic
Space group	$P2_1$	$P2_12_12_1$	$P2_1$	$P1$	$C2$	$C2$	$P2_1$	$P2_1$	$P2_12_12_1$
a, b, c/nm	1.3365(4)	2.0698(2)	0.98080(5)	0.79550(2)	1.73260(4)	3.15910(6)	1.01680(8)	1.6428(4)	0.75000(1)
	1.1036(4)	2.8908(3)	1.09010(4)	1.23980(4)	1.13690(3)	1.08750(2)	0.80240(6)	0.7794(4)	0.83290(1)
	1.9880(4)	1.1465(1)	2.1211(2)	1.80350(4)	1.73950(4)	1.70050(2)	2.29470(19)	2.3465(4)	4.33190(4)
α, β, γ/°	90	90	90	98.980(2)	90	90	90	90	90
	94.05(2)	90	95.211(2)	99.526(2)	116.838(2)	101.092(1)	90.000(4)	104.988(16)	90
	90	90	90	101.012(2)	90	90	90	90	90
Volume/nm^3	2.9249(14)	6.8599(15)	2.28879(17)	1.68922(8)	3.05738(13)	5.73297(10)	1.8722(3)	2.902(2)	2.70603(5)
T/K	293(2)	293(2)	100(2)	100(2)	100(2)	200(2)	100(2)	293(2)	100(2)
Z	2	4	2	2	4	8	2	4	4
μ/mm^{-1}	0.130 (Mo–K_α)	1.079 (Cu–K_α)	1.282 (Cu–K_α)	1.288 (Cu–K_α)	1.455 (Cu–K_α)	1.399 (Cu–K_α)	1.447 (Cu–K_α)	0.155 (Mo–K_α)	1.480 (Cu–K_α)
Reflections measured,	7372	5855	19180	16949	11879	25256	15080	7376	24965
unique (*R*int)	7074	5014	5625	7067	3592	10061	3317	7133	4159
	(0.0048)	(0.067)	(0.034)	(0.030)	(0.032)	(0.038)	(0.032)	(0.029)	(0.035)
R_1	0.0525	0.0807	0.1089	0.0857	0.0533	0.0768	0.0809	0.0454	0.0416
R_{all}	0.0995	0.0891[b]	0.1122[c]	0.0883[c]	0.0534	0.0776[c]	0.0858[c]	0.1288	0.0422

[a] The solvent molecules were included in the crystal structure. [b] Disorder of ethyl acetate molecules were observed and restrained. [c] Disorder of alkylsilyl moieties were observed and restrained.

Table 2 Average of isotropic thermal parameters of non-hydrogen atoms, geometrical details of the tape motif packing structures in the alkylsilylated nucleoside crystals and thermal properties (DSC) of these crystals

Crystal	Average of U_{iso} of base/ribose/ alkylsilyl moieties	Inter-base distance/nm	Tape-tape distance/nm		Tape motif assembly	Temperature of endothermic peak/°C
			Intra-layer	Inter-layer		
1a·MeOH	0.044/0.042/0.079	1.147	1.337	1.988	**WL**	51–81 (MeOH)[e], 200.9, 268.1 (mp)
1a·EA	0.061/0.058/0.120	1.104	(2.070, 1.778)[d]		**H**	54–83 (2EA)[e], 230.8, 267.0 (mp)
1b	0.073/0.100/0.195	1.090	0.981	2.121	**WL**	240 (decomp)
1c·MEK[a]	0.023/0.028/0.042	1.148	(1.933, 1.338)[d]		**H**	84.9–87.7 (MEK)[e], 280 (decomp)
1c·MeOH[a]	0.061/0.063/0.135	1.288[c]	0.968	1.674	**L**	30–79.3 (MeOH)[e], 86, 260 (decomp)
2b	0.033/0.038/0.085	0.796[b]	1.240	1.804	**L**	199.2, 298 (decomp)
2c·AcOH	0.021/0.028/0.047	1.137	0.866	1.552	**L**	121.7 (AcOH)[e], 138.7, 280 (decomp)
3a[a]	0.039/0.041/0.059	1.108	0.953	1.971	**WL**	79.0, 250 (decomp)
3b[a]	0.019/0.023/0.041	1.121	0.851	1.841	**L**	200 (decomp)
3c	0.046/0.064/0.115	1.088	0.850	1.580	**L**	260 (decomp)
4	0.040/0.041/0.066	0.802	1.017	2.295	**WL**	116.7, 141.7 (mp)
5	0.053/0.056/0.112	0.779	1.173	1.643	**L**	117.8, 180 (mp)
6	0.025/0.025/0.037	0.833	0.832	2.166	**L**	129.8 (mp)

[a] Our previous studies.[11,14,17] [b] Short inter-base distance of other hydrogen-bonded network. [c] Long inter-base distance of hydrogen-bonded network containing methanol molecule. [d] Tape–tape distances in the H structure. [e] Evaporation of inclusion molecules.

of their low molecular symmetry, we successfully obtained crystals suitable for single crystal X-ray analysis from all the alkylsilylated nucleosides. Crystallisation of **1a** and **1c** from different solvents gave two different crystals, **1a·MeOH** and **1a·EA**, and **1c·MeOH** and **1c·MEK**, respectively. The crystal structures of the alkylsilylated nucleosides were successfully obtained by X-ray diffraction measurements. Crystallographic data of the newly-analysed six guanosine derivatives and three adenosine derivatives are listed in Table 1. Together with four crystal structures that have been reported previously,[11,14a,17] a total of ten and three crystal structures of the alkylsilylated guanosine and adenosine derivatives, respectively, are available.

For **1b**, **2b**, **3c**, and **4**, notable disorders were observed in the alkylsilyl moieties, which resulted in higher R_1 values even after suitable restraints were applied. Temperature factors of the atoms in the base, ribose, and alkylsilyl moieties were averaged respectively, and are listed in Table 2. Larger average values for the alkylsilyl moiety might reflect the disorders or small displacements arising from the flexible nature of these moieties.

Hydrogen-bonded tape motif in the alkylsilylated nucleoside crystal

Hydrogen-bonded tape motifs were found in all the alkylsilylated nucleoside crystals. Except for **1c·MeOH**[17] and **2b**, the tape motifs found in the guanosine derivatives were constructed by the typical hydrogen-bonding pattern shown in Fig. 1(a). Double hydrogen bonds between adjacent guanine moieties, 1-NH ··· 7-N and 2-(NH)H ··· 6-O, stretched along the crystal axis to form the tape motifs. The inter-base distances in these tape motifs were 1.088–1.147 nm (Table 2), which are comparable to those reported for other guanine derivatives.[18,19] Additional hydrogen bond formation was also noticed in many of the crystals. In addition to the tape motif formation, one of the amino hydrogens (2-NH_2) was hydrogen-bonded to the incorporated solvent molecule (**1c·MEK**[11] and **2c·AcOH**), or to the phenyl group of TBDPS to form H-π hydrogen bonds (**1a·MeOH** and **1a·EA**). The hydrogen bond network of **1a·EA** is shown in Fig. 2a as a typical example. In the case of **3b**[14a] and **3c**, additional double inter-tape hydrogen bonds were formed between 2-NH_2 and 3-N of the two guanine-bases located in the adjacent tape motifs, leading to the formation of the two-dimensional hydrogen-bonded layer structure (Fig. 2b shows the hydrogen bond pattern of **3c**). Unlike eight other crystals, **1c·MeOH** and **2b** had different hydrogen-bonded tape motifs. In the **2b** crystal (Fig. 2c), one of the amino hydrogens (2-NH_2) and the ring amide hydrogen (1-NH) formed two hydrogen bonds with the adjacent guanine carbonyl oxygen (6-O), and the other amino hydrogen (2-NH_2) with the other guanine (7-N). In addition, an intra-molecular hydrogen bond was formed between ribose 5′-OH and guanine 3-N. While, in the case of **1c·MeOH**,[17] one of the methanol molecules in the crystal participated in the hydrogen-bonding network of the tape motif (Fig. 2d), which increased the inter-base distance (d) to 1.288 nm.

The alkylsilylated adenosines had the same hydrogen-bonding pattern in their crystals, the 6-NH ··· 1-N and 6-NH ··· 7-N double hydrogen bonds that are commonly observed in the crystals of adenine derivatives. The inter-base distances in these tape motifs were 0.779–0.833 nm (Table 2), which coincided well with the reported distances of adenine derivatives.[20,21] Within the **5** crystal, two slightly different tapes were found. Ribose 5′-OH formed an additional hydrogen bond with 3-N of the adjacent adenine in an *anti* conformation in one of the tapes (Fig. 3a), but with 7-N of the same molecule in a *syn* conformation in the other tape (Fig. 3b).

Packing pattern of hydrogen-bonded tape motifs in the crystals

The packing mode of the hydrogen-bonded tape motifs in the alkylsilylated guanosine crystals is shown in Fig. 4. In all the crystals, the tape motifs were found to stretch along the crystal axis, the perpendicular direction to the plane in Fig. 4. In the **2c·AcOH**, **3b**[14a] and **3c** crystals, the hydrogen-bonded tape motifs aligned side by side to form two-dimensional layers, which were piled up to become a lamella-like (**L**) structure (Fig. 4a and 4b). Within the layer, the guanine moiety and the alkylsilyl groups constituted separate domains and the polar guanine domain was sandwiched by the non-polar alkylsilyl domains. In the case of the latter two, adjacent tape motifs within the layer were connected by the additional inter-tape hydrogen bonds. A similar packing mode of the tape motifs was found in the **1c·MeOH** and **2b** crystals, though their hydrogen-bonding patterns of the tape motifs were different.

In the **1a·MeOH** (Fig. 4e), **1b** (Fig. 4d) and **3a**[14a] crystals, the non-polar and bulky alkylsilyl groups surrounded the hydrogen-bonded guanine tape moieties. The tape motifs were aligned to form the layered structures in the crystals. However, the guanine moiety of the each tape motif within the layer was separated by the alkylsilyl groups, and no direct contact was observed between the polar guanine domains of the adjacent tapes. Since the packing mode can be expressed as an expanded or widened lamellar-like structure, we designated this packing mode as the **WL** structure, while, in the **1a·EA** (Fig. 4f) and **1c·MEK**[11] crystals, the tape motifs were packed into herring-bone-like **H** structures.

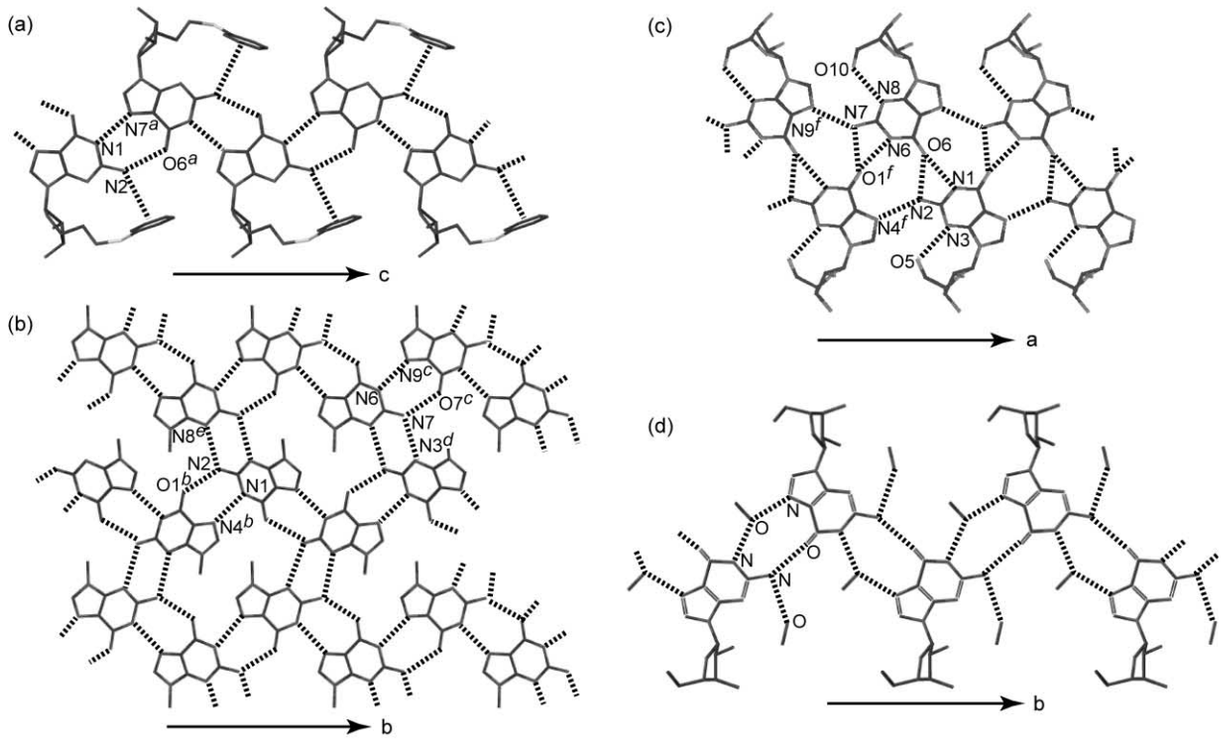

Fig. 2 Hydrogen-bonded tape motifs in **1a·EA** (a), **3c** (b), **2b** (c), and **1c·MeOH** (d). Alkylsilyl groups, hydrogen atoms and sugar moieties in (b) were omitted for clarity. Hydrogen bonds are indicated as dotted lines. Symmetry codes: [a] 1/2 − x, −y, 1/2 + z; [b] 3/2 − x, −1/2 + y, 1 − z; [c] 3/2 − x, 1/2 + y, −z; [d] x, 1 + y, z; [e] x, −1 + y, z; [f] −1 + x, y, z.

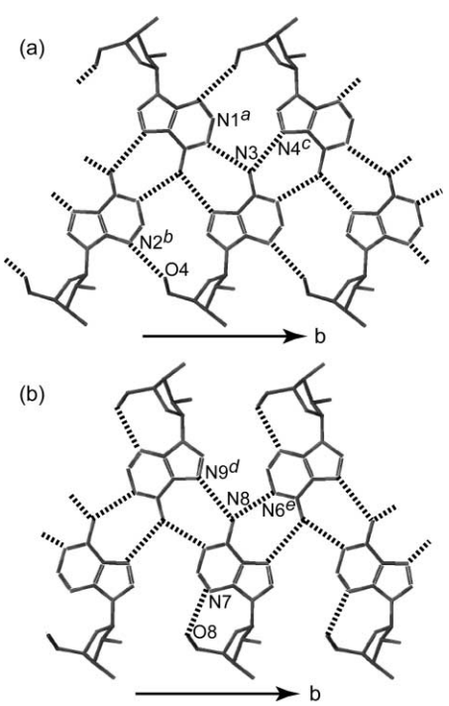

Fig. 3 Hydrogen-bonded tape motifs in **5** of the anti comformers (a) and syn comformers (b). Alkylsilyl groups and hydrogen atoms were omitted for clarity. Hydrogen bonds are indicated as dotted lines. Symmetry codes: [a] −1 − x, −1/2 + y, −1 − z; [b] x, −1 + y, z; [c] −1 − x, 1/2 + y, −1 − z; [d] −1 − x, −1/2 + y, −z; [e] −1 − x, 1/2 + y, −z.

The tape motifs of alkylsilylated adenosines were also packed into either the **L** or **WL** structures depending on their constituents. In the case of the **5** and **6** crystals having two alkylsilyl moieties, their tape motifs formed the lamella-like **L** structure, while the tape motifs of **4** having three side chains were packed into the **WL** structure (Fig. 5).

The tape–tape distances between or within the layer(s) in the **L** and **WL** structures are listed in Table 2. For the **H** structures, two inter-tape distances are listed in parentheses due to the rectangular packing within the plane perpendicular to the tape axis.

Thermal analysis of alkylsilylated nucleoside crystals

The thermal properties of the crystals were analysed by DSC and TG. Melting or decomposition temperatures of the guanosine derivatives were above 200 °C, showing high stability of these compounds. Endothermic peaks observed in the DSC curves at the first heating process are also listed in Table 2. The crystals incorporating solvent molecules showed additional endothermic peaks, which were ascribed to the release of the entrapped solvent molecules based on the observed weight loss at the corresponding temperatures in TG. Some of the crystals having no solvent molecules also showed additional endothermic peaks presumably due to solid–solid phase transitions, and these peaks were confirmed to be reproducible by reheating. Since the characteristic hydrogen-bonded amino and carbonyl peaks were observed in the IR spectra of the TBDMS-substituted derivatives heated above the transition temperatures, the hydrogen-bonded tape motifs were preserved even above the transition temperatures. The observed solid–solid phase transition could be attributed to the partial melting of the flexible and non-polar alkylsilyl moieties.

Discussion

Role of the adjustable unit and structural hierarchy in the crystals

Substrates with low molecular symmetry are difficult to crystallise. Indeed, only 27 crystal structures of guanosine derivatives (excluding mixtures, metal complexes and polynucleotides) are reported in the Cambridge Structural Database.[23] In this study, all eight alkylsilylated guanosines having different numbers and types of nonpolar and flexible alkylsilyl side chains were crystallised from appropriate solvents, suggesting that crystallisation of these compounds took place without any difficulty.

Together with those of the adenosine derivatives, a total of thirteen crystal structures are available. The molecular struc-

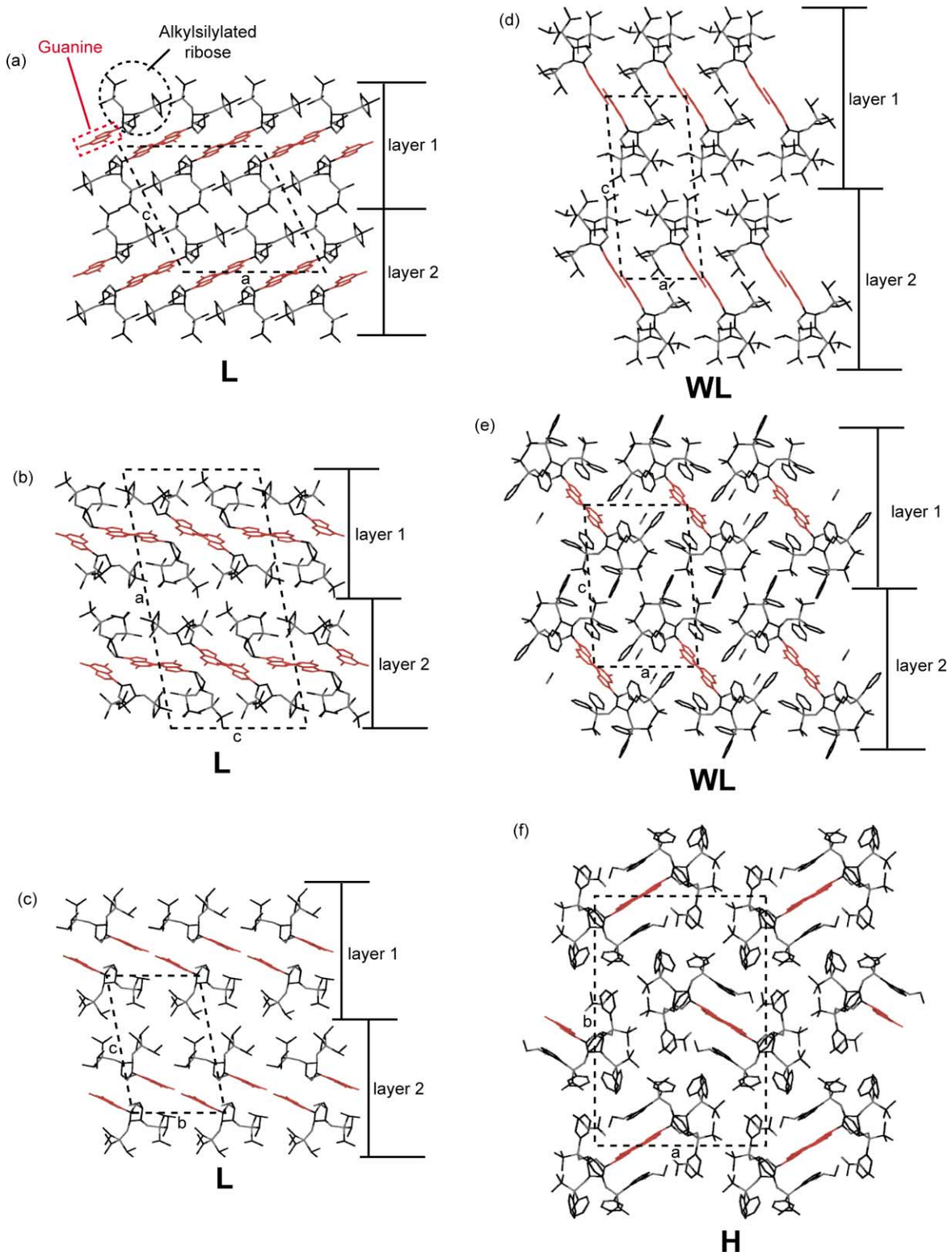

Fig. 4 Tape motif packing structures of **2c·AcOH** (a), **3c** (b), **2b** (c), **1b** (d), **1a·MeOH** (e), and **1a·EA** (f). Disorder parts were represented as the parts of largest occupancy and hydrogen atoms were omitted for clarity.

tures of these compounds are composed of two different moieties, the guanine or adenine moiety as the hydrogen-bonding site to form the robust tape motifs and the alkylsilylated ribofuranose moiety as the adjustable soft segment. The use of different numbers and types of alkylsilyl side chains caused appreciable difference in shape and size of the latter unit. Except for **1c·MeOH** and **2b**, however, these crystals preserved the one-dimensional tape motifs formed by the typical hydrogen-bonding patterns for either guanine or adenine derivatives. Therefore, the structural hierarchy found in the gels, fibres and films[11,14] were also recognised in these crystals, suggesting that these tape motifs acted as sufficiently robust building blocks.

On the other hand, the flexible alkylsilylated ribose moiety seemed to show a buffer or a filling effect to assist the packing of the robust tape motifs to achieve the closest packing required for the crystallisation. Indeed, a variety of ribofuranose puckering patterns and $O_{4'}$–$C_{1'}$–N_9–C_4 dihedral angles (χ) found in these crystals (Table 3) allowed large conformational diversity in the moieties. In addition, notable disorders and the large temperature factors were found in the alkylsilyl domains, which might reflect their flexible nature. This view is further supported

Table 3 *N*-glycosyl bond dihedral angle and ribose puckering in the alkylsilylated nucleoside crystals

Crystal	O4′–C1′–N1–C4 dihedral angle (χ)/°	Ribose puckering[a]	V_{adj}/V_{base}	Packing coefficient (C_k*)[b]
WL structure				
1a·MeOH	64.05	$^{2}\mathbf{T}_{3}$	7.77[c]	0.549
1b	73.06	$^{2}\mathbf{T}_{3}$	5.89	0.552
3a	−163.09	$_{3}\mathbf{T}^{2}$	5.23	0.550
4	79.06	$^{3}\mathbf{E}$	4.88	0.535
H structure				
1a·EA	72.98	$^{2}\mathbf{T}_{3}$	9.00[c]	0.531
1c·MEK	64.61	$^{2}\mathbf{T}_{3}$	5.26[c]	0.583
L structure				
1c·MeOH	−137.06	$^{2}\mathbf{E}$	3.72[c,d]	0.565
2b	66.42, 59.69	$^{2}\mathbf{T}_{3}$, $^{2}\mathbf{T}_{3}$	4.28	0.572
2c·AcOH	−121.08	$^{2}\mathbf{T}_{3}$	3.83[c]	0.580
3b	−55.91, −167.69	$^{3}\mathbf{E}$, $^{3}\mathbf{E}$	4.24	0.587
3c	−102.71, −168.49	$^{2}\mathbf{T}_{3}$, $^{3}\mathbf{E}$	3.28	0.548
5	58.71, −147.10	$^{2}\mathbf{T}_{3}$, $^{2}\mathbf{T}_{3}$	3.60	0.535
6	120.62	$_{2}\mathbf{E}$	3.53	0.574

[a] Ribose puckering; Envelope form $^{2}\mathbf{E}$: 2′-endo, $^{3}\mathbf{E}$: 3′-endo, $_{2}\mathbf{E}$: 2′-exo; Twist form $^{2}\mathbf{T}_{3}$: 2′-endo-3′-exo, $_{3}\mathbf{T}^{2}$: 3′-exo-2′-endo. [b] $C_k^* = Z(V_m/V_c)$, where Z is the number of the molecules in the unit cell, V_m is the volume of the molecule and V_c is the volume of the unit cell. [c] The volume V_{adj} included the incorporated solvent molecules. [d] The volume V_{base} included one methanol molecule.

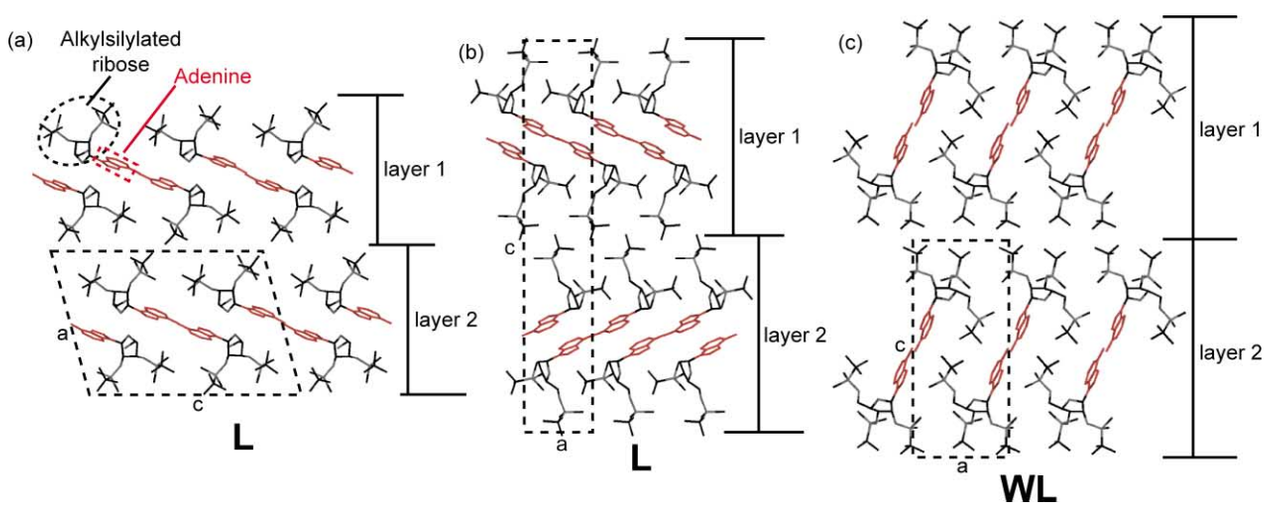

Fig. 5 Tape motif packing structures of **5** (a), **6** (b) and **4** (c). Disorder parts were represented as the parts of largest occupancy and hydrogen atoms were omitted for clarity.

by the observed solid–solid phase transition suggesting partial melting of these moieties. Thus, all the alkylsilylated nucleosides were successfully assembled into crystals suitable for X-ray analysis, showing that the molecular design using an adjustable soft segment as a molecular pad is an effective method for crystal engineering of the robust hydrogen-bonded tape motifs.

As mentioned above, **1c·MeOH** and **2b** crystals had different hydrogen-bonded tape motifs. In the case of **2b**, 5′-OH was hydrogen-bonded to the guanine N3. In the **1c·MeOH** crystal, one of the methanol molecules was hydrogen-bonded with the adjacent guanine N7 and N1 to form the tape motif of a different hydrogen-bonding pattern, while **1c·MEK** formed the typical tape motif. These results suggest that the presence of an extra hydrogen-bond donor might cause disruption of the hydrogen-bonding pattern of the tape motif in some cases, though the tape motifs of **1a·MeOH** and **2c·AcOH** showed the typical hydrogen-bonding pattern.

Packing mode of the tape motifs

Molecular packing is the critical process in crystallisation, therefore, molecular shape significantly affects the crystal structure. On the other hand, the role of the alkylsilylated ribose moieties as the molecular pad in crystal packing might be understood in terms of their molecular size instead of their molecular shape because of their high adjustable nature. Therefore, a rationally defined structural parameter to access the relative size of the soft segment will allow us to evaluate and possibly predict the crystal structure of the hydrogen-bonded tape motifs. It is well recognised that "the critical packing parameter" of amphiphiles is a useful measure to understand and predict their mode of aggregation from the molecular structure.[24] The parameter is defined as a relative volume of the hydrophobic chain of the amphiphile molecule to a volume projected by the optimal head group area, and the structure of the aggregate varies from spherical or cylindrical micelles, vesicles or bilayers, to reversed micelles as the parameter increases. We adopted a similar but simpler parameter as a measure of the relative size of the soft segment. The dimensionless parameter is defined as V_{adj}/V_{base}, the volume of the adjustable alkylsilylated ribofuranose moiety V_{adj} relative to that of the nucleobase moiety V_{base}. The volumes V_{adj} and V_{base} were determined from their van der Waals volumes in optimised geometry. When the solvent molecules are incorporated in the crystals, their van der Waals volumes are included in either V_{adj} or V_{base} depending on the location of the solvent molecules. The calculated parameters are listed in Table 3. When the relative

volume of the adjustable unit is below 4.28, the tape motifs are packed in the lamellar-like **L** structure, while they are packed into **H** or **WL** structure when the parameter is larger than 4.56. In the case of **1c**, the **1c·MEK** crystal composed of the typical hydrogen-bonded tape motifs has the **H** structure, whose parameter is 5.26, while for the **1c·MeOH** crystal which has the lamellar-like **L** structure, the parameter becomes 3.72. These results demonstrate that the relative volume (V_{adj}/V_{base}) of the adjustable segment can be used as an effective measure to understand and predict the packing mode of the hydrogen-bonded tape motifs.

Packing coefficients C_k* of the crystals are also listed in Table 3. This coefficient represents the extent of the volume of the molecules in the unit cell, and higher packing is generally preferred.[25] However, the coefficients of the crystals packed in the **L** structure are in the range between 0.548 and 0.587, while those of the crystals in the **H** or **WL** structure are from 0.531 to 0.583, and practically no difference is noticed. Therefore, the packing coefficient is not an effective measure for the packing mode of the tape motifs.

Thus, the packing mode of the hydrogen-bonded tape motifs is successfully explained by the relative volume of the adjustable unit without taking into account their molecular shape, which further confirms the role of the nonpolar and adjustable alkylsilylated ribose moieties as the molecular pad in crystal packing.

Conclusion

In this study, we examined crystals of eleven alkylsilylated nucleoside derivatives having different numbers and types of non-polar and flexible alkylsilyl side chains. For all the compounds, we successfully obtained their crystals from appropriate solvents in spite of their low molecular symmetry. In these crystals, the tape motifs are formed by the inter-base hydrogen bonds, and they are arranged either in the **L**, **H** or **WL** structure in the crystals. However, the alkylsilylated ribose unit has a variety of conformations with notable disorders at the alkylsilyl moiety. Therefore, the role of the adjustable and nonpolar alkylsilyl ribose unit is to provide cushioning or a filling effect as the molecular pad in the packing of the robust hydrogen-bonded tape motifs at crystallisation. The role of the adjustable unit as the molecular pad is further supported by the fact that the packing mode of the tape motifs in the crystal can be interpreted by the relative volume of the adjustable unit. Thus, a novel molecular design using the adjustable unit as the molecular pad offers a unique approach to the crystal engineering of the mesoscopic-scale predicted and self-assembled motifs.

Experimental

Preparation of the alkylsilylated nucleoside crystals

Alkylsilylated nucleosides were synthesised by using the corresponding trialkylchlorosilane and imidazole in DMF according to the method of Ogilvie *et al.*[26] or Furuta *et al.*,[27] and their molecular structures and abbreviations are shown in Scheme 1. **1a** and **2b** were newly synthesised. Crystallisation was carried out by slowly evaporating the solvents over a period of a week at room temperature. Suitable single crystals of alkylsilyl nucleosides were obtained from the solvents listed in Table 1.

2′,3′,5′-Tris-*O*-(tert-butyldiphenylsilyl)guanosine (1a). ^{1}H-NMR (400 MHz, $CDCl_3$) δ 1.0 (27H), 3.13 (1H, dt), 3.53 (1H, dt), 4.12 (1H, dd), 4.71 (1H, dd), 4.85 (2H, br), 4.99 (1H, dd), 6.02 (1H, d), 7.3 (30H), 7.74 (1H, s), 12.01 (1H, br); FAB MS *m*/*z* 999 ([MH$^+$] $C_{58}H_{67}N_5O_5Si_3$ requires 999).

2′,3′-Bis-*O*-(triisopropylsilyl)guanosine (2b). ^{1}H-NMR (400 MHz, $CDCl_3$) δ 0.69–1.62 (41H), 3.67–3.94 (2H, m), 4.13–4.16 (1H, m), 5.16 (1H, dd), 5.65 (1H, d), 6.49 (3H, m), 7.46 (1H, s), 12.15 (1H, br); FAB MS *m*/*z* 596 ([MH$^+$] $C_{28}H_{53}N_5O_2$ requires 596).

Crystallography

For crystallographic data collection ‡, a MacScience DIP-Labo or MXC18 with graphite-monochromatized Cu-Kα radiation, or a Rigaku AFC7r with graphite-monochromatized Mo-Kα radiation was used. Calculations were performed using maXus[28] or teXsan[29] crystallographic software packages. The crystal structures were solved by direct method using SIR92[30] or Shelxs-97[31] and the structure refinements were performed by a full-matrix least squares methods using Shelxl-97.[31] Details of the data are summarised in Table 1. The solvent molecules were included in the crystals of **1a·EA** (two ethyl acetate molecules in asymmetric unit), **1a·MeOH** (methanol) and **2c·AcOH** (acetic acid). Disorders of alkylsilyl groups were observed in **1b**, **2b**, **3c** and **4** crystals, to which suitable restraints were applied and refined isotropically. In the **1a·EA**, two ethyl acetate molecules were disordered intricately, to which similar restraints were applied. The methanol molecule in **1a·MeOH** and a part of a phenyl group in **1a·EA** were suggested to have disorder, however, we could not construct a suitable disorder model. Then, we refined them isotropically. Other non-hydrogen atoms were refined anisotropically. Hydrogen atoms of the solvent molecules in **1a·MeOH** and **1a·EA** were omitted, and other hydrogen atoms were placed at idealised geometry.

Thermal analysis

Differential scanning calorimetry (DSC) and thermogravimetry (TG) were carried out with a Rigaku DSC 8230 and TG-DTA 8120, respectively. The crystal samples of about 5 mg were measured at a heating rate of 5 °C min^{-1}. The samples that showed any phase transition in DSC measurements were cooled down slightly before starting decomposition and were subjected to re-heating in order to test their reproducibility.

Molecular structure analysis

To understand the structural features, the molecular structures of the alkylsilylated nucleosides were further analysed by the Insight II[32] molecular modelling program package on a SGI O_2. The volume of the adjustable unit (V_{adj}) and base moiety (V_{base}) was determined from the alkylsilylated ribose moiety and nucleobase moiety's van der Waals volume in optimised geometry by the CFF/Discover force field.

Acknowledgements

This study was partly supported by a Grant-in-Aid for Scientific Research (No. 14350482 and No. 14045211) from the Ministry of Education, Science, Sports, and Culture, Japan.

‡ CCDC reference numbers 225956–225964. See http://www.rsc.org/suppdata/ob/b3/b315769e/ for crystallographic data in .cif or other electronic format.

References

1 (*a*) E. Weber, *Design of organic solids, Topics in Current Chemistry*, Springer-Verlag, New York, 1998; (*b*) G. R. Desiraju, *Crystal Engineering, The design of organic solids*, Elsevier, Amsterdam, 1989.
2 (*a*) J. Perlstein, *J. Am. Chem. Soc.*, 1992, **114**, 1955; (*b*) A. Gavezzotti, G. Filippini, J. Kroon, B. P. van Eijck and P. Klewinghaus, *Chem. Eur. J.*, 1997, **3**, 893; (*c*) J. P. M. Lommerse, W. D. S. Motherwell, H. L. Ammon, J. D. Dunitz, A. Gavezzoti, D. W. M. Hofmann, F. J. J. Leusen, W. T. M. Mooij, S. L. Price, B. Schweizer, M. U. Schmidt, B. P. van Eijck, P. Verwer and D. E. Williams, *Acta Crystallogr., Sect. B: Struct. Sci.*, 2000, **56**, 697.
3 (*a*) G. M. Whitesides, J. P. Mathias and C. T. Seto, *Science*, 1991, **254**, 1312; (*b*) T. Shimizu, *Macromol. Rapid Commun.*, 2002, **23**, 311.

4 (*a*) G. R. Desiraju, *Angew. Chem., Int. Ed. Engl.*, 1995, **34**, 2311; (*b*) G. R. Desiraju, *Chem. Commun.*, 1997, 1475; (*c*) J. C. MacDonald and G. M. Whitesides, *Chem. Rev.*, 1994, **94**, 2383; (*d*) S. Coe, J. J. Kane, T. L. Nguyen, L. M. Toledo, E. Wininger, F. W. Fowler and J. W. Lauher, *J. Am. Chem. Soc.*, 1997, **119**, 86; (*e*) B. Moulton and M. J. Zaworotko, *Chem. Rev.*, 2001, **101**, 1629.

5 (*a*) M. C. Etter, *Acc. Chem. Res.*, 1990, **23**, 120; (*b*) J. Bernstein, R. E. Davis, L. Shimoni and N. –L. Chang, *Angew. Chem., Int. Ed. Engl.*, 1995, **34**, 1555.

6 S. Palacin, D. N. Chin, E. E. Simanek, J. C. MacDonald, G. M. Whitesides, M. T. McBride and G. T. R. Palmore, *J. Am. Chem. Soc.*, 1997, **119**, 11807.

7 L. J. Williams, B. Jagadish, S. R. Lyon, R. A. Kloster, M. D. Carducci and E. A. Mash, *Tetrahedron*, 1999, **55**, 14281.

8 (*a*) L. J. Williams, B. Jagadish, M. G. Lansdown, M. D. Carducci and E. A. Mash, *Tetrahedron*, 1999, **55**, 14301; (*b*) B. Jagadish, L. J. Williams, M. D. Carducci, C. Bosshard and E. A. Mash, *Tetrahedron Lett.*, 2000, **41**, 9483.

9 D. N. Chin, G. T. R. Palmore and G. M. Whitesides, *J. Am. Chem. Soc.*, 1999, **121**, 2115.

10 K. N. Ganesh, V. A. Kumar, D. A. Barawkar, in *Supramolecular Control of Structure and Reactivity*, ed. A. D. Hamilton, John Wiley & Sons Ltd., 1996, pp. 263–327.

11 K. Araki, R. Takasawa and I. Yoshikawa, *Chem. Commun.*, 2001, 1826.

12 G. Gottarelli, S. Masiero, E. Mezzina, S. Pieraccni, J. P. Rabe, P. Samori and G. P. Spada, *Chem. Eur. J.*, 2000, **6**, 3242.

13 T. Giorgi, F. Grepioni, I. Manet, P. Mariani, S. Masiero, E. Mezzina, S. Pieraccni, L. Saturni, G. P. Spada and G. Gottarelli, *Chem. Eur. J.*, 2002, **8**, 2143.

14 (*a*) T. Sato, M. Seko, R. Takasawa, I. Yoshikawa and K. Araki, *J. Mater. Chem.*, 2001, **11**, 3018; (*b*) I. Yoshikawa, J. Li, Y. Sakata and K. Araki, *Angew. Chem., Int. Ed.*, 2004, **43**, 100.

15 (*a*) M. Gellert, M. N. Lipsett and D. R. Davies, *Proc. Natl. Acad. Sci. USA*, 1962, **48**, 2013; (*b*) A. L. Marlow, E. Mezzina, G. P. Spada, S. Masiero, J. T. Davis and G. Gottarelli, *J. Org. Chem.*, 1999, **64**, 5116; (*c*) S. L. Forman, J. C. Fettinger, S. Pieraccini, G. Gottarelli and J. T. Davis, *J. Am. Chem. Soc.*, 2000, **122**, 4060.

16 W. Saenger, *Principles of Nucleic Acid Structure*, Springer-Verlag, New York, 1984.

17 K. Araki, M. Abe, A. Ishizaki and T. Ohya, *Chem. Lett.*, 1995, 359.

18 Guanine derivatives: (*a*) W. M. Macintyre, P. Singh and M. S. Werkema, *Biophys. J.*, 1965, **5**, 697; (*b*) G. I. Birnbaum, M. Cygler and D. Shugar, *Can. J. Chem.*, 1984, **62**, 2646; (*c*) S. Fujita, A. Takenaka and Y. Sasada, *Bull. Chem. Soc. Jpn.*, 1984, **57**, 1707; (*d*) R. Destro, T. J. Kistenmacher and R. E. Marsh, *Acta Crystallogr., Sect. B: Struct. Crystallogr. Cryst. Chem.*, 1974, **30**, 79; (*e*) S. Oouchi, A. Takenaka and Y. Sasada, *Acta Crystallogr., Sect. C: Cryst. Struct. Commun.*, 1986, **42**, 1340; (*f*) G. I. Birnbaum, N. G. Johansson and D. Shugar, *Nucleosides Nucleotides*, 1987, **6**, 775; (*g*) U. Thewalt, C. E. Bugg and R. E. Marsh, *Acta Crystallogr., Sect. B: Struct. Crystallogr. Cryst. Chem.*, 1971, **27**, 2358.

19 Guanosine derivatives: (*a*) C. C. Wilson, J. N. Low and P. Tollin, *Acta Crystallogr., Sect. C: Cryst. Struct. Commun.*, 1985, **41**, 1123; (*b*) J. N. Low, P. Tollin, C. C. Wilson and S. N. Scrimgeour, *Acta Crystallogr., Sect. C: Cryst. Struct. Commun.*, 1986, **42**, 700; (*c*) S. S. Mande, T. P. Seshadri and M. A. Viswamitra, *Acta Crystallogr., Sect. C: Cryst. Struct. Commun.*, 1988, **44**, 912; (*d*) U. Thewalt, C. E. Bugg and R. E. Marsh, *Acta Crystallogr., Sect. B: Struct. Crystallogr. Cryst. Chem.*, 1970, **26**, 1089; (*e*) L. H. Koole, H. M. Buck, J. A. Kanters and A. Schouten, *Can. J. Chem.*, 1988, **66**, 2634; (*f*) P. van Roey and C. K. Chu, *Nucleosides Nucleotides*, 1992, **11**, 1229; (*g*) S. S. Mande, T. P. Seshadri and M. A. Viswamitra, *Acta Crystallogr., Sect. C: Cryst. Struct. Commun.*, 1989, **45**, 92.

20 Adenine derivatives: (*a*) S. J. Cline and D. J. Hodgson, *Biochim. Biophys. Acta*, 1979, **563**, 540; (*b*) S. J. Cline and D. J. Hodgson, *Biochim. Biophys. Acta*, 1980, **610**, 20; (*c*) S. Sugio, H. Mizuno, K. Kitamura, K. Hamada, M. Ikehara and K. -I Tomita, *Acta Crystallogr., Sect. C: Cryst. Struct. Commun.,*, 1983, **39**, 745; (*d*) S. Sugio, H. Mizuno, K. Kitamura, K. Hamada, M. Ikehara and K. -I. Tomita, *Acta Crystallogr., Sect. C: Cryst. Struct. Commun.*, 1984, **40**, 712; (*e*) M. Kamimura, A. Takenaka, Y. Sasada and M. Ohki, *Acta Crystallogr., Sect. C: Cryst. Struct. Commun.*, 1986, **42**, 601; (*f*) T. Kaneda and J. Tanaka, *Bull. Chem. Soc. Jpn.*, 1976, **49**, 1799; (*g*) G. Bunick and D. Voet, *Acta Crystallogr., Sect. B: Struct. Sci.*, 1982, **38**, 575; (*h*) G. S. D. King, *J. Chem. Res.*, 1981, **121**, 1501; (*i*) M. Bohringer, H. -J. Roth, J. Hunziker, M. Gobel, R. Krishnan, A. Giger, B. Schweizer, J. Schreiber, C. Leumann and A. Eschenmoser, *Helv. Chim. Acta*, 1992, **75**, 1416; (*j*) D. Scharfenberg-Pfeiffer, R. -G. Kretschmer and S. Hoffmann, *Cryst. Res. Technol.*, 1988, **23**, 881; (*k*) S. M. Tret'yak, V. V. Mitkevich and L. F. Sukhodub, *Kristallografiya*, 1990, **35**, 365; (*l*) A. K. Das, S. K. Mazumdar, N. Das, S. K. Talapatra and A. J. van Aerschot, *Crystallogr. Spectrosc. Res.*, 1993, **23**, 177; (*m*) B. Doboszewski, N. Blaton and P. Herdewijn, *J. Org. Chem.*, 1995, **60**, 7909; (*n*) A. Takenaka, M. Shibata and Y. Sasada, *Acta Crystallogr., Sect. C: Struct. Commun.*, 1986, **42**, 1336; (*o*) A. Alexandrescu, W. B. Drendel and M. Sundaralingam, *Acta Crystallogr., Sect. C: Struct. Commun.*, 1991, **47**, 1041; (*p*) T. J. Kistenmacher and M. Rossi, *Acta Crystallogr., Sect. B: Struct. Crystallogr. Cryst. Chem.*, 1977, **33**, 253.

21 Adenosine derivatives: (*a*) W. S. Sheldrick and M. Morr, *Acta Crystallogr., Sect. B: Struct. Crystallogr. Cryst. Chem*, 1980, **36**, 2328; (*b*) B. Dimke and E. Liebigs, *Ann. Chem.*, 1983, 1409; (*c*) M. M. Radwan, *Acta Crystallogr., Sect. B: Struct. Crystallogr. Cryst. Chem*, 1980, **36**, 2185; (*d*) S. Neidle, *Acta Crystallogr., Sect. B: Struct. Crystallogr. Cryst. Chem*, 1979, **35**, 708; (*e*) C. C. Wilson, P. Tollin and R. A. Howie, *Acta Crystallogr., Sect. C: Struct. Commun.*, 1986, **42**, 697; (*f*) D. G. Watson, D. J. Sutor and P. Tollin, *Acta Crystallogr.*, 1965, **19**, 111; (*g*) L. H. Koole, *Can. J. Chem.*, 1987, **65**, 326; (*h*) L. H. Koole, H. M. Buck, J. A. Kanters and A. Schouten, *Acta Crystallogr., Sect. C: Struct. Commun.*, 1987, **43**, 1370; (*i*) J. N. Low, P. Tollin and R. A. Howie, *Acta Crystallogr., Sect. C: Struct. Commun.*, 1987, **43**, 2184; (*j*) A. Matsuda, H. Kosaki, Y. Saitoh, Y. Yoshimura, N. Minakawa and H. Nakata, *J. Med. Chem.*, 1998, **41**, 2676; (*k*) D. Prahadee, *Acta Crystallogr., Sect. C: Struct. Commun.*, 1999, **55**, 389; (*l*) P. J. Bolon, T. B. Sells, Z. M. Nuesca, D. F. Purdy and V. Nair, *Tetrahedron*, 1994, **50**, 7747; (*m*) D. Prahadee, *Acta Crystallogr., Sect. C: Struct. Commun.*, 1999, **55**, 606; (*n*) S. Sprang, *Acta Crystallogr., Sect. B: Struct. Crystallogr. Cryst. Chem.*, 1978, **34**, 2803; (*o*) V. M. Vrudhu, *J. Med. Chem.*, 1989, **32**, 885; (*p*) T. Fujii, T. Saito and T. Date, *Chem. Pharm. Bull.*, 1989, **37**, 1208; (*q*) P. Prusinerand and M. Sundaralingam, *Acta Crystallogr., Sect. B*, 1976, **32**, 161; (*r*) N. L. H. L. Broeders, A. P. van der Heiden, L. H. Koole, J. A. Kanters and A. Schouten, *Can. J. Chem.*, 1993, **71**, 855; (*s*) L. H. Koole, S. Neidle, M. D. Crawford, A. A. Krayevski, G. V. Gurskaya, A. Sandstrom, J. -C. Wu, W. Tong and J. Chattopadhyaya, *J. Org. Chem.*, 1991, **56**, 6884; (*t*) P. Singh and D. J. Hodgson, *Acta Crystallogr., Sect. B: Struct. Crystallogr. Cryst. Chem.*, 1979, **35**, 973.

22 C. Rucker, *Chem. Rev.*, 1995, **95**, 1009.

23 F. H. Allen, *Acta Crystallogr.,Sect. B: Struct. Sci.*, 2002, **58**, 380.

24 J. N. Israelachvili, *Intermolecular and Surface Forces*, Academic Press, London, 1985.

25 A. I. Kitaigorodskii, *Physical Chemistry Vol.29: Molecular Crystals and Molecules*, Academic Press, New York, 1973.

26 (*a*) K. K. Ogilvie, *Can. J. Chem.*, 1973, **51**, 3799; (*b*) K. K. Ogilvie, S. L. Beaucage, A. L. Schifman, N. Y. Theriault and K. L. Sadana, *Can. J. Chem.*, 1978, **56**, 2768; (*c*) K. K. Ogilvie, A. L. Schifman and C. L. Penney, *Can. J. Chem.*, 1979, **57**, 2230.

27 H. Furuta, K. Furuta and J. L. Sessler, *J. Am. Chem. Soc.*, 1991, **113**, 4706.

28 S. Mackay, C. J. Gilmore, C. Edwards, N. Stewart and K. Shankland, maXus, Cumputer Program for the Solution and Refinement of Crystal Structures, Nonius, The Netherlands, MacScience, Japan, The University of Glasgow.

29 teXsan, Computer Program for the Solution and Refinement of Crystal Structures, Rigaku, Japan.

30 SIR92: A. Altomare, M. C. Burla, M. Camalli, G. Cascarano, C. Giacovazzo, A. Guagliardi and G. Polidori, *J. Appl. Crystallogr.*, 1994, **27**, 435.

31 G. M. Sheldrick, SHELX-97, Program for the Solution and Refinement of Crystal Structures, University of Göttingen, Germany, 1997.

32 Insight II 98 molecular modeling program package, Biosym/MSI, San Diego, 1998.